

Deriving Information about Architecture from Activity Patterns in Coupled Cell Systems*

Krešimir Josić[†] and Jonathan Rubin[‡]

Abstract. In coupled networks, the properties of the constituent elements (cells), their interactions, and the coupling architecture combine to determine the possible coherent states that may arise. In this work, we examine what can be said about the coupling architecture of a network based on an observed polysynchronous activity pattern, in which cells form multiple synchronized clusters. Specifically, we derive a linear relation, the solutions of which are precisely those coupling architectures that are robustly compatible with a given polysynchronous state. We analyze this relation under the assumption that the network consists of either a ring of identical cells or a double ring of two interacting cell populations. Comparison of these cases shows that coupling of an “observed” layer of cells to a second “hidden” layer can significantly broaden the range of architectures that support certain clustering patterns in the observed cells.

Key words. network coupling architecture, polysynchronous states, balanced coloring

AMS subject classifications. 05C40, 34C14, 34C15, 37C80

DOI. 10.1137/040607587

1. Introduction. The phenomenon of spontaneous synchronization in networks of coupled systems is ubiquitous in nature and has been studied in a variety of settings [20, 25]. Many of the theoretical studies of the phenomenon start by postulating models for the individual systems and their interactions in the network. The collective behavior of the network is then analyzed after a particular pattern of connections, or coupling architecture, has been specified. The properties of the individual systems, their interactions, and the coupling architecture are all important in determining the features of the coherent states that appear in such networks.

The present work provides a different approach to the analysis of synchrony in networks. Rather than specifying the properties of the network at the outset, we assume that a particular activity pattern has been observed in the network, but little else is known. The question we begin to address is the following: Can one infer anything about the network’s coupling architecture from the fact that it supports the observed mode of activity? More specifically, we ask how a network’s capability to produce a particular activity pattern constrains the possible coupling architectures that may be present in the network.

The problem of constructing a network architecture that produces a certain activity pattern has been considered, for instance, to construct networks that can serve as central pattern

*Received by the editors April 4, 2004; accepted for publication (in revised form) by D. Terman August 11, 2004; published electronically February 22, 2005. This work was supported in part by NSF grants DMS-0244529, DMS-0108857, and DMS 0414023 (to Rubin).

<http://www.siam.org/journals/siads/4-1/60758.html>

[†]Department of Mathematics, University of Houston, Houston, TX 77204-3008 (josic@math.uh.edu).

[‡]Department of Mathematics and Center for the Neural Basis of Cognition, University of Pittsburgh, Pittsburgh, PA 15260 (rubin@math.pitt.edu).

generators for the various gaits observed in quadrupeds [12, 11]. The approach used in these studies was based on the analysis of the symmetries of the system, which lead to the spatiotemporal patterns of activity corresponding to different gaits. In the present work, we study *polysynchronous* states, featuring multiple synchronized clusters that may be out of synch with each other. Although polysynchronous states may result from the symmetries of a network, as studied, for example, by Pogromsky, Santoboni, and Nijmeijer [21], such states may not have the full symmetries of the network, and they may also appear in networks that do not possess any symmetries. In general, while it is clear that there is a connection between patterns of synchrony in a network and the network architecture, the relation between the two has, up to this point, been poorly understood.

In contrast to [12, 11, 21], the mathematical methods introduced in this paper rely on local information about architecture and can thus be used to analyze states that do not result from global symmetries of the network. We apply these methods to fully analyze which architectures are compatible with specified polysynchronous states. Examples of synchronous patterns that are not due to symmetry have also been discussed in [10], and we provide a general framework for analyzing the networks that can support such patterns. One direct consequence of this analysis is the result that the presence of a “hidden” layer of cells can strongly impact the range of network architectures that can support a given activity pattern in an “observed” layer of cells.

A significant motivation for studying architectural implications of coherent activity states derives from the field of neuroscience. Experimental and computational evidence suggests that synchronized activity of synaptically interconnected neuronal ensembles contributes to a variety of cognitive tasks, such as attending to regions in the receptive field [9] and recognizing learned spatiotemporal patterns [15, 16]. Moreover, the power of synchronized neuronal oscillations at various frequencies is augmented during certain periods or states, as in cortical gamma rhythms during epochs of attentiveness associated with successful learning [9, 17], thalamic spindle and delta rhythms during periods of sleep [7, 8], and subthalamopallidal oscillations in parkinsonian states (reviewed in [3]). Note that synchronized states relevant to the above examples include states of polysynchrony.

Through biophysically based computational modeling of neuronal networks, one can attempt to assess the contributions of various features of intrinsic and synaptic dynamics to the occurrence of synchronized states. Computational results also highlight the crucial role that the synaptic architecture, or pattern of synaptic connections between neurons, can play in shaping network behavior (e.g., [26]); indeed, changes in synaptic architecture alone can induce significant changes in firing patterns within a model neuronal network. Unfortunately, experimental information about synaptic architectures, particularly the architecture of effective synapses in a network, is sketchy in many cases. In particular, while it may be possible to ascertain that two general brain areas are synaptically connected (e.g., from viral injection studies [14]), it is much more difficult to establish details about synaptic density, reciprocity, or patterning. Given these difficulties, a theoretical means to infer information about the synaptic architecture of a network from the nature of experimentally observed activity patterns in a network would represent a valuable tool in the analysis and computational modeling of neuronal networks. Importantly, such an inverse approach could also be used to constrain the range of synaptic architectures to be considered in simulations of a network known to

generate certain dynamics.

In this work, we take an abstract, model independent approach to the inverse problem of using a network’s activity patterns to constrain its coupling architecture. Although we consider only states of exact polysynchrony, the conclusions we obtain are not restricted to any particular type of system. While all patterns of synchrony can be observed in an all-to-all coupled network, we will seek to specify *all* of the architectures that can *robustly* yield given activity patterns. Here, robustness refers to the fact that with these architectures, changes in the intrinsic dynamics of its components will not destroy the specified patterns (as long as the changes are made so that cells in the network which are assumed to be equal remain equal). To focus our investigation, we will assume that the network coupling architecture features \mathbf{Z}_N symmetry (for arbitrary fixed population size N). This means that if we index the cells by the integers $0, \dots, N-1$, and then shift all indices up by the same positive integer $(\text{mod } N-1)$, then for any $i, j \in \{0, \dots, N-1\}$, the number of connections from cell i to cell j is not changed by this shift. Networks with this symmetry are typically referred to as rings, and we will generally think of the cells in the network as forming a ring for convenient visualization in the figures. This is the approach taken in many computational studies of waves, localized activity, and other organized activity patterns in discrete models of neuronal networks as well. Note, however, that the actual spatial arrangement of cells in a network under study is irrelevant, as the symmetry here relates only to the coupling architecture, and that the methods we present will apply in the absence of \mathbf{Z}_N symmetry as well.

We emphasize that we consider the mathematical ideal of synchrony: If x_0 and x_1 are the state variables of two systems, then the systems are synchronous only if $x_0 = x_1$. Implicitly, we will make an even stronger assumption. Given a system of N cells described by internal variables x_0, \dots, x_{N-1} , each evolving in state space \mathbf{R}^m , two systems x_i and x_j will be able to exhibit synchronous behavior only if the manifold $S_{i,j} = \{(x_0, \dots, x_{N-1}) \in \mathbf{R}^m : x_i = x_j\}$ contains an invariant submanifold. This is a strong assumption, which may not cover all situations of interest in practice. However, such an assumption is desirable, because if invariant manifolds corresponding to synchronous behavior exist and are stable in an appropriate sense,¹ then the synchronous states persist under small perturbations away from synchrony.

An example of the type of solution we seek is given in Figure 1. Here, a polysynchronous state is specified by coloring the cells according to their cluster membership; i.e., cells sharing the same color are synchronous. Our results yield constraints on the set of all inputs to each cell in the network. When these constraints are satisfied, the input sets for different cells of the same color are equivalent. This means that all cells of the same color receive the same number of inputs from cells in different clusters. We refer to a coloring of a network with this property as a *balanced coloring* and define it mathematically in section 2.2 below. Figure 1 illustrates an architecture that achieves a balanced coloring, although it is not the only such architecture. We will show that, without assuming the existence of a layer of I cells (the rectangular cells in the figure), only a network with all-to-all coupling can support the 2-cluster polysynchronous pattern in the E cells shown in Figure 1. Therefore, the existence of a “hidden” layer of cells allows for a much sparser network architecture, such as that shown in Figure 1.

In the next section, we give a more thorough introduction of the notation and terminology,

¹In fact, normal hyperbolicity is necessary and sufficient.

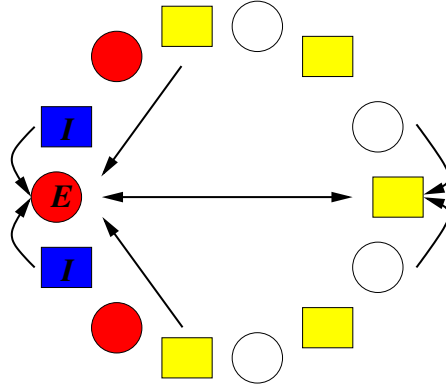


Figure 1. An example of a balanced coloring with E cell clusters of sizes 3 and 4, and I cell clusters of sizes 2 and 5, achieved within a double ring. The connection pattern shown repeats for all cells in the network, such that each red E cell receives inputs from 2 blue I cells and 3 yellow I cells; each white E cell receives inputs from 1 blue I cell and 4 yellow I cells; each blue I cell receives inputs from 2 red E cells and 1 white E cell; and each yellow I cell receives inputs from 1 red E cell and 2 white E cells.

such as the notions of an input set and a balanced coloring. Further, we derive the general mathematical formulation of the architectural specification problem that we will consider. In section 3, we state and prove our first main result, on architectures that support 2-cluster solutions on a ring. We also present an example of the application of our result to a particular solution and ring, and we discuss general ways to check the connectedness of architectures. In section 4, we state and prove our second main result, on polysynchronous solutions in rings of two cell types, providing an example of how the presence of a second cell type can weaken strict architectural constraints that would be required for certain activity patterns to arise in a ring of just one cell type. We conclude with a discussion in section 5.

2. Notation and mathematical description of the problem. The main idea of our approach is to translate the problem of constructing an architecture that allows for certain patterns of polysynchrony into the problem of finding integer solutions to a set of linear equations. In this section, we introduce notation and illustrate our approach in a simple example.

2.1. Polysynchrony in a small example network. For simplicity, we first consider networks of identical cells, so that each cell evolves in the same phase space as the others. The *connectivity matrix* A of the network is a matrix of nonnegative integers, where an entry $a_{i,j}$ denotes the number of connections from cell j to cell i . We assume that the connections between the cells in the network are identical to avoid introducing multiple connectivity matrices. Figure 2 provides an example of a six cell network, with \mathbf{Z}_6 symmetry, along with its connectivity matrix. Note that due to the \mathbf{Z}_6 symmetry, if we increment (mod 6) all cell labels in Figure 2 by a fixed positive integer, then the connection matrix A will not change.

The structure of a network has to be reflected in the equations that are used to model it. In particular, if the internal states of the cells in the network of Figure 2 are denoted by $x_i \in \mathbf{R}^k$ for $i = 0, \dots, 5$, and we set $x = (x_0, x_1, x_2, x_3, x_4, x_5)$, then a differential equation modeling the evolution of this network must have the form

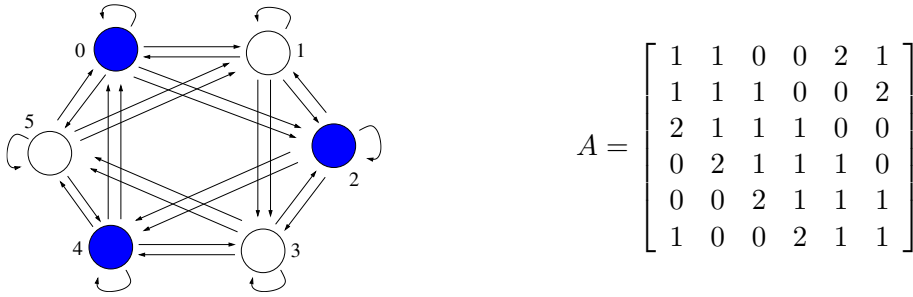


Figure 2. An example of a network of six identical cells and its connectivity matrix.

$$(2.1) \quad \begin{aligned} x'_0 &= f(x_0, x_1, x_4, x_4, x_5), & x'_3 &= f(x_3, x_4, x_1, x_1, x_2), \\ x'_1 &= f(x_1, x_2, x_5, x_5, x_0), & x'_4 &= f(x_4, x_5, x_2, x_2, x_3), \\ x'_2 &= f(x_2, x_3, x_0, x_0, x_1), & x'_5 &= f(x_5, x_0, x_3, x_3, x_4). \end{aligned}$$

To obtain system (2.1), we assume that for any fixed $j \in \{0, \dots, 5\}$, the effect of the input from cell $i + j \pmod{5}$ to cell i , $i = 0, \dots, 5$, is independent of i (see [13] for a formal treatment).

It can be checked by direct substitution that the linear submanifolds $\mathcal{X} = \{x : x_i = x_j \text{ for all } i \text{ and } j\}$ and $\mathcal{Y} = \{x : x_0 = x_2 = x_4 \text{ and } x_1 = x_3 = x_5\}$ are invariant under the evolution of system (2.1); i.e., solutions with initial conditions in \mathcal{X} and \mathcal{Y} remain in \mathcal{X} and \mathcal{Y} , respectively, for all time. Therefore, any differential equation model of the network given in Figure 2 supports both the fully synchronous state $x = (x(t), x(t), x(t), x(t), x(t), x(t))$ and the polysynchronous state $x = (x_0(t), x_1(t), x_0(t), x_1(t), x_0(t), x_1(t))$.

We note that the *existence* of these states is a consequence only of the assumed network architecture (in this case, the \mathbf{Z}_N symmetry of the network). Other features, such as the stability of the synchronous states, depend on the details of the model's dynamics.

2.2. Polysynchronous states in general networks. It is natural to ask what polysynchronous states a given network architecture can support. This problem has been explored in detail in [24, 13]. Our present goal is to provide a general approach to answering the inverse question: Given a particular polysynchronous state, what are the network architectures that can support it? In this section we introduce the notation we use to describe a general polysynchronous state and the conditions on the network architecture that allow the network to support such states.

To describe a pattern of polysynchrony in a network of N cells, we first number the cells in the network. To do so, we assign integer indices $i = 0, 1, \dots, N - 1$ to the cells. We start with 0 here and throughout the paper for convenience in calculations using modular arithmetic. Each cell is then assigned a vector $c_i \in \mathbf{R}^m$, where m is the number of synchronous clusters that appear in the polysynchronous solution of interest. Each c_i will be a unit vector from the standard basis $\{e_0, \dots, e_{m-1}\}$ for \mathbf{R}^m , and the position of the nonzero element of the vector will denote which group of synchronous cells the cell i belongs to. Therefore, cell i is synchronous with cell j if and only if $c_i = c_j = e_l$ for some $l \in \{0, \dots, m - 1\}$.

Let $\mathcal{C}_i = \{i_0, \dots, i_{k-1}\}$ and $\mathcal{C}_j = \{j_0, \dots, j_{l-1}\}$ be the collections of cells that provide inputs to cells i and j , respectively, or their *input sets*. If a single cell provides n inputs to

cell i , it is listed n times in \mathcal{C}_i . It is shown in [24, 13] that two cells in a network can be expected to display *robust* synchrony, such that synchrony persists under small changes in cellular dynamics that preserve network architecture, only if their input sets are identical. More precisely, the cells i and j can be expected to be robustly synchronous only if there exists a bijection $\phi : \mathcal{C}_i \rightarrow \mathcal{C}_j$ such that if $\phi(i_r) = j_q$, then $c_{i_r} = c_{j_q}$; under this condition, ϕ maps input cells from any fixed synchronous group to input cells from the same synchronous group.

The existence of the bijection ϕ between the input sets of two cells means that the two cells receive the same number of inputs from each of the synchronous clusters. Suppose we color all cells in a network, such that all cells in a synchronous cluster share the same color, with different colors for different clusters. If for every pair of cells in the same cluster, i.e., of the same color, there exists such a bijection, then such a coloring is referred to as *balanced* [24, 13]. A balanced coloring ensures that polysynchronous states are robust, in the sense described above, as stated in the following result.

Theorem 2.1 (see [24, 13]). *A coloring is balanced if and only if the corresponding polysynchronous state is robust.*

This observation can be translated into an equation by using the notation established above. Let $\sum_{k=0}^{N-1} a_{i,k} c_k = R_i$, so that R_i is the m -vector whose l th entry is equal to the number of inputs cell i receives from the synchronous cluster l . The requirement that the cells i and j have the same input set is equivalent to the requirement that

$$(2.2) \quad \sum_{k=0}^{N-1} a_{i,k} c_k = R_i = R_j = \sum_{k=0}^{N-1} a_{j,k} c_k.$$

Remark 2.1. In the mathematical neuroscience literature, the architectures assumed for the analytical study of polysynchronous states are generally relatively simple and do yield balanced colorings. An interesting example appears in [26], where a balanced coloring is achieved with the architecture that yields robust polysynchrony of clusters in an E-I network, the so-called structured, sparsely connected architecture.

Now, set $c = [c_0, \dots, c_{N-1}]^T \in \mathbf{R}^{mN}$, representing a pattern of synchrony. Using (2.2), the problem of finding an architecture such that the coloring associated with the specified polysynchronous m -cluster state is balanced becomes the problem of finding a connectivity matrix $A \in \mathbf{R}^{N \times N}$ and a vector $R = [R_0, \dots, R_{N-1}]^T \in \mathbf{R}^{mN}$, both with nonnegative integer entries, such that

$$(2.3) \quad (A \otimes I_m)c = R.$$

In (2.3), I_m is the m by m identity matrix and \otimes denotes the tensor product.

A more geometric interpretation of this condition is the following: Let \mathcal{R}_c be the linear subspace of \mathbf{R}^{mN} defined by $\mathcal{R}_c = \{R = (R_0, R_1, \dots, R_{N-1}) \in \mathbf{R}^{mN} : R_i = R_j \text{ whenever } c_i = c_j\}$. Equation (2.3) implies that the problem of finding a network architecture that supports a given pattern of synchrony c is equivalent to finding a matrix A that maps the given pattern of synchrony c to a point in \mathcal{R}_c with nonnegative integer components. Note that \mathcal{R}_c has dimension m^2 since each of the m synchronous clusters is characterized by a

corresponding m -vector. Note further that it does not matter *which* point in \mathcal{R}_c is attained; the important point is to find an A such that $(A \otimes I_m)c$ is in \mathcal{R}_c .

Example. Consider a *ring* of four cells, denoted by c_0, \dots, c_3 . Suppose that we want to find an architecture that supports two synchronized clusters, in which cells 0 and 1 share one color and cells 2 and 3 share another. Following the notation above, we set

$$c_0 = c_1 = \begin{bmatrix} 1 \\ 0 \end{bmatrix} \text{ and } c_2 = c_3 = \begin{bmatrix} 0 \\ 1 \end{bmatrix}.$$

Our assumption that we are dealing with a ring of cells means that the network has \mathbf{Z}_4 symmetry when the coloring is not taken into account (see Figure 3). As a consequence, the matrix A is circulant, so that

$$A = \begin{bmatrix} a_0 & a_1 & a_2 & a_3 \\ a_3 & a_0 & a_1 & a_2 \\ a_2 & a_3 & a_0 & a_1 \\ a_1 & a_2 & a_3 & a_0 \end{bmatrix}.$$

The condition that the coloring is balanced is equivalent to requiring that the following equations can be satisfied by some nonnegative integers a_0, a_1, a_2, a_3 and 2-vectors of nonnegative integers R and S

$$(2.4) \quad \begin{aligned} a_0c_0 + a_1c_1 + a_2c_2 + a_3c_3 &= R, & a_2c_0 + a_3c_1 + a_0c_2 + a_1c_3 &= S, \\ a_3c_0 + a_0c_1 + a_1c_2 + a_2c_3 &= R, & a_1c_0 + a_2c_1 + a_3c_2 + a_0c_3 &= S. \end{aligned}$$

Through a simple manipulation of (2.4) we obtain the system of equations

$$(2.5) \quad \begin{aligned} a_0 + a_1 &= R_0, & a_2 + a_3 &= R_1, \\ a_3 + a_0 &= R_0, & a_1 + a_2 &= R_1 \end{aligned}$$

and four more redundant equations. These equations imply $a_1 = a_3$, while a_0 and a_2 are arbitrary. R and S are determined once the values of a_0 , $a_1 = a_3$, and a_2 are set. The value of a_0 describes the coupling of a cell to itself, and can be thought of as one of a cell's intrinsic characteristics.

The three possibilities with single arrows between cells, and $a_0 = 0$, are shown in Figure 3. Note that when $a_1 = a_2 = a_3 = 1$ we have all-to-all coupling. Since any coloring will be balanced for such a coupling, this solution is uninteresting. Moreover, when $a_1 = a_3 = 0$ and $a_2 = 1$ (Figure 3C), the network consists of two disconnected subnetworks. We also consider such solutions uninteresting. Therefore the only nontrivial solution in this example is given by $a_1 = a_3 = 1$, and $a_2 = 0$, as in Figure 3B.

Remark 2.2. To keep the exposition concise, we do not deal with networks in which all cells and connections are not identical, such as neuronal networks with multiple forms of neurotransmitters and receptors. The precise relation between the network architecture and the structure of the system of equations that models the network, as well as the machinery necessary to analyze this relation, is introduced in [24, 13].

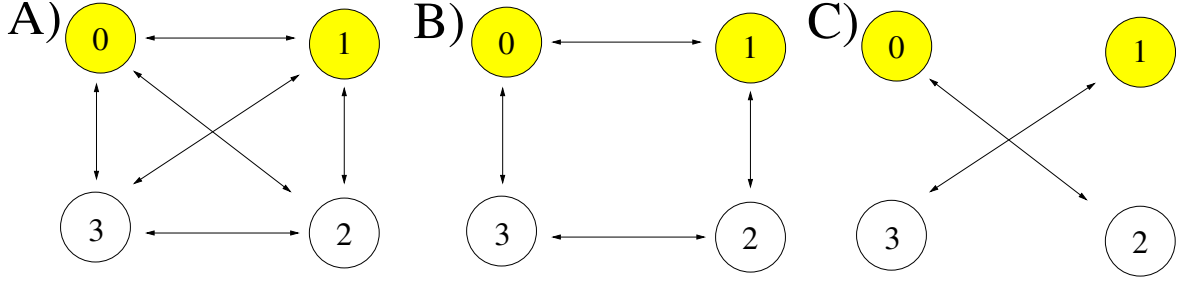


Figure 3. Three possible architectures with single arrows leading to a balanced coloring in a ring with the synchrony pattern described in the text. From left to right, (a) $a_1 = a_2 = a_3 = 1$, (b) $a_1 = a_3 = 1$, $a_2 = 0$, (c) $a_1 = a_3 = 0$, $a_2 = 1$. In all cases $a_0 = 0$, corresponding to no self-coupling.

The reader may have noticed that the connectivity matrices for the networks given in Figures 3B and 3C sum to give the connectivity matrix of the network in Figure 3A. This is a consequence of the following general result.

Proposition 2.2. *The set of matrices $\mathcal{A}_c = \{A \in \mathbf{Z}^{N \times N} : A \text{ satisfies (2.3) for some } R \in \mathcal{R}_c\}$ forms a module over the integers.*

Proof. Suppose that A and B satisfy (2.3) for $R^A \in \mathcal{R}_c$ and $R^B \in \mathcal{R}_c$, respectively, and a fixed c . If cells i and j are synchronous, then

$$(2.6) \quad \sum_{k=0}^{N-1} a_{i,k} c_k = R_i^A = R_j^A = \sum_{k=0}^{N-1} a_{j,k} c_k$$

and similarly for B and R^B . Therefore $kA + lB$ satisfies (2.3) with the input vector $kR^A + lR^B$. Since \mathcal{R}_c is a linear subspace, it contains $kR^A + lR^B$. ■

Remark 2.3. The subset of the module \mathcal{A}_c consisting of matrices with nonnegative entries is the set of all connectivity matrices that satisfy (2.3) for some $R \in \mathcal{R}_c$.

Note that matrix \mathbf{O} with all entries equal to 1; i.e., $[\mathbf{O}]_{i,j} = 1$ for all i, j , is in \mathcal{A}_c for any c . Therefore any polysynchronous solution is supported in an all-to-all coupled network. Suppose that $A \in \mathcal{A}_c$ represents a network with at most single connections between cells. Then $\bar{A} = \mathbf{O} - A$ is in \mathcal{A}_c , and represents another network with at most single connections between cells. We call \bar{A} the *complement* of A and refer to the two networks whose connectivities are given by matrices A and \bar{A} as *complementary networks*. In particular, the networks given in Figures 3B and 3C are complementary networks.

2.3. Restrictions on architecture. With no restrictions on the matrix A , the problem of solving (2.3) for a given pattern of synchrony c is not interesting. Both an all-to-all coupled network and a network in which all cells are only coupled with themselves support all patterns of synchrony, and the problem becomes trivial in these cases.

Another type of trivial solution is provided by a disconnected network. Consider the network shown in Figure 4. This 9-cell network supports a polysynchronous solution with clusters of 3 and 6 cells. Upon closer inspection (Figure 4B), one can see that this network is really a union of 3 equal networks of 3 cells. We consider such solutions trivial, since there are no interactions between the cells in the separate networks, and therefore the synchronous states cannot be robust.

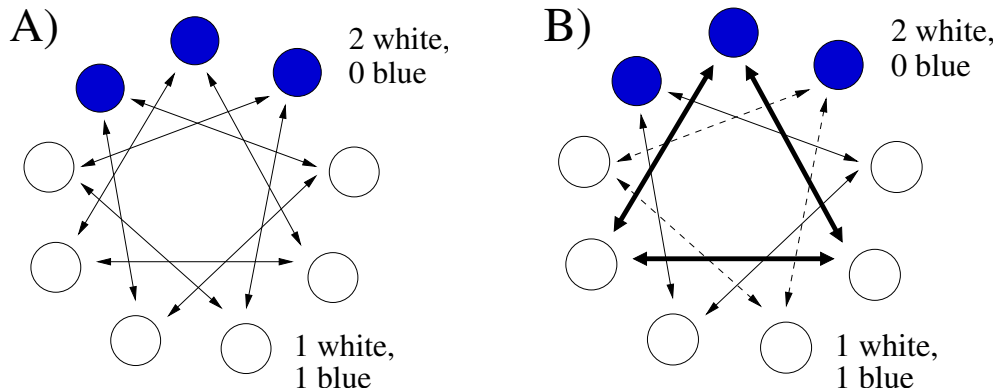


Figure 4. A balanced coloring for a 2-cluster solution in a network of nine cells. The text in this and subsequent figures indicates the numbers of connections to each cell of each type. On the right, we have used three different arrow types to emphasize that this architecture consists of three disconnected components.

In contrast to these trivial architectures, naturally occurring networks are frequently observed or assumed to have a certain nontrivial but patterned structure, which is reflected in the coupled cell systems used to model them. If we assume certain reasonable restrictions on the structure of the networks under consideration, the problem of constructing an architecture that supports a given pattern of synchrony becomes more interesting and informative. As discussed in the introduction, ring architectures are ubiquitous in models of neuronal networks, as well as models of other systems. Therefore, in the following, as in the example above, we consider networks of cells with \mathbf{Z}_N symmetry.

The approach we describe here can be directly extended beyond this case. It is important, however, to specify a class of architectures at the outset, to avoid an overabundance of solutions. A restriction on architecture can be given by imposing a certain symmetry of the architecture, as we have done, or it could be made more general [24, 13]. The constraint used here translates into a constraint on the connectivity matrix A . With this constraint, the problem consists of finding solutions of (2.2) within the specified class of connectivity matrices given a particular polysynchronous pattern.

In section 3, we will consider 2-cluster polysynchronous solutions in rings of one cell type. We will assume that the members of any fixed cluster are adjacent in the network (with adjacency defined in terms of connections, not necessarily spatial location). In section 4, we consider multicluster solutions in a pair of interacting rings, exemplified by a network in which cells of two types are interleaved. Although the framework and ideas used in the two sections are similar, the double ring structure will require more careful analysis.

In the neuronal context, interactions of cells of two distinct, spatially intermingled types are of particular interest because local neuronal circuits *in vivo* commonly consist of interacting excitatory (E) and inhibitory (I) populations, such as thalamocortical relay (E) and thalamic reticular (I) cells in the thalamus, the subthalamic nucleus (E) and the globus pallidus (I) in the basal ganglia, and pyramidal cells (E) and interneurons (I) in most cortical areas. Note that the theory we develop, even in the case of rings of one cell type, allows for different types of connections, such as excitatory and inhibitory or fast and slow, between cells, as long as connections emanating from all cells within a single cluster are of the same type.

In terms of the coupled cell formalism that we employ, the fact that a network consists of multiple cell types means that the cells of different type cannot belong to the same synchronous cluster and therefore cannot share the same color. While the same conditions could be obtained by restricting the patterns of synchrony that can occur in such networks, it is conceptually simpler to postulate the existence of different types of cells.

One interesting result that arises from our approach is that, in some cases where rings of identical cells can only support patterns of synchrony if the network is equipped with a trivial (uncoupled or all-to-all coupled) architecture, the presence of two types of cells (such as the E and I cells discussed above) can greatly broaden the range of architectures that support polysynchronous states.

Example. Consider a ring of 7 E cells shown in Figure 1. It follows from Corollary 3.3, proved in the next section, that solutions with synchronous clusters of 2 and 5 cells, or of 3 and 4 cells, require all-to-all coupling.

Suppose that we instead consider a ring consisting of alternating E and I cells. While the dynamics of the I cells may or may not be of interest in their own right, we shall see that it is important to take their presence into account when analyzing E cell activity.

In a network of 7 E cells alternating with 7 I cells, it is possible to produce a nontrivial balanced coloring of four colors with clusters of sizes 3 and 4 (E cell clusters) and 2 and 5 (I cell clusters); see Figure 1 for an example. This balance is achieved by an architecture in which each E cell sends connections to its nearest neighbors (which are I cells) and to the I cell directly across the ring from itself, while each I cell sends connections to its nearest neighbors (which are E cells), to its next-nearest neighbor E cells, and to the E cell directly across the ring. This result does not require any E-E or I-I connections but will be preserved under the inclusion of all-to-all E-E and/or I-I connections, based on Corollary 3.3.

Thus, the presence of a “hidden” layer of cells can allow for particular polysynchronous solutions to emerge in an “observed” layer of cells, even though it would not be possible to obtain these same patterns with a nontrivial architecture in a ring of just a single cell type. We emphasize that, although there are no E-E or I-I connections, this architecture is nontrivial due to the connections between the cells of different types. Although the E cells do not interact directly in such a network, their activity is shaped by their indirect interactions through the I cells.

3. Rings of cells with two synchronous clusters. In this section we assume that the architecture of a network of N identical cells has \mathbf{Z}_N symmetry, so that the cells form a ring. We assume that two groups of adjacent cells form synchronous clusters and we answer the question: What architectures support the given pattern of synchrony?

The assumption of \mathbf{Z}_N symmetry implies that the connectivity matrix A is circulant. We could refer to the well-studied properties of circulant matrices to slightly shorten the discussion that follows [6]. In fact, using the particular structure of the equations, a trick can be used to solve them directly, as will be shown in the proof of Theorem 4.1. However, we take a more general approach because the ideas used will also apply whenever the network is assumed to be Γ symmetric,² for an abelian group Γ . In this situation the irreducible representations of Γ

²We hope that similar ideas are also applicable when “symmetries” of the system are given by a groupoid, rather than a group [24]. Unfortunately, a representation theory of groupoids that would be applicable to such examples does not seem to have been developed yet.

can be used to diagonalize the connectivity matrix A in the way illustrated below.

3.1. Setup and main result. Consider a ring of N cells that is separated into two groups of adjacent cells of sizes k and $N - k$. The k cells in the first group are numbered 0 through $k - 1$, while cells in the second group are numbered k through $N - 1$. Following the notation introduced in section 2.2, we have $c_0 = \cdots = c_{k-1} = \begin{bmatrix} 1 \\ 0 \end{bmatrix}$ and $c_k = \cdots = c_{N-1} = \begin{bmatrix} 0 \\ 1 \end{bmatrix}$.

As shown in section 2.2, the problem of finding an architecture that supports this pattern of synchrony reduces to finding a connectivity matrix A that satisfies (2.3) with $m = 2$. Under the assumption that the cells form a ring, (2.3) has the form

$$(3.1) \quad \begin{array}{ll} a_0 + a_1 + \cdots + a_{k-1} = R_0 & a_k + a_{k+1} + \cdots + a_{N-1} = R_1 \\ a_{N-1} + a_0 + \cdots + a_{k-2} = R_0 & a_{k-1} + a_k + \cdots + a_{N-2} = R_1 \\ \cdots & \cdots \\ a_{N-k+1} + a_{N-k+2} + \cdots + a_0 = R_0 & a_1 + a_2 + \cdots + a_{N-k} = R_1 \\ a_{N-k} + a_{N-k+1} + \cdots + a_{N-1} = S_0 & a_0 + a_1 + \cdots + a_{N-k-1} = S_1 \\ a_{N-k-1} + a_{N-k} + \cdots + a_{N-2} = S_0 & a_N + a_0 + \cdots + a_{N-k-2} = S_1 \\ \cdots & \cdots \\ a_1 + a_2 + \cdots + a_k = S_0 & a_{k+1} + a_{k+2} + \cdots + a_0 = S_1. \end{array}$$

It is straightforward to check, by subtracting successive equations, that the equations in the left and right columns of (3.1) are equivalent. We will therefore deal only with the equations in the left column. To simplify computations, we reorder these equations, putting the first equation first, and then following with the last equation up to the second equation, although this step is not essential.

Once reordered, these equations can be written as

$$(3.2) \quad Ma = R,$$

where $a = (a_0, a_1, \dots, a_{N-1})^T$ and

$$R = (R_0, \underbrace{S_0, \dots, S_0}_{N-k \text{ times}}, R_0, \dots, R_0)^T.$$

Here

$$(3.3) \quad M = \begin{bmatrix} 1 & 1 & 1 & \cdots & 1 & 0 & 0 & \cdots & 0 & 0 \\ 0 & 1 & 1 & \cdots & 1 & 1 & 0 & \cdots & 0 & 0 \\ 0 & 0 & 1 & \cdots & 1 & 1 & 1 & \cdots & 0 & 0 \\ & & & \cdots & & & & \cdots & & \\ 1 & 1 & 1 & \cdots & 0 & 0 & 0 & \cdots & 0 & 1 \end{bmatrix},$$

where each row contains $N - k$ zero entries.

Since we are not fixing the value of R (rather, it is determined after the coefficients in a are set), the problem of interest is equivalent to finding all vectors of positive integers a such that

$$(3.4) \quad Ma \in V,$$

where

$$V = R_0 w_1 \oplus S_0 w_2 \stackrel{\text{def}}{=} R_0(1, 1, 1, \dots, 1)^T \oplus S_0(1, 0, 0, \dots, 0, 1, 1, \dots, 1)^T.$$

This problem is solved in the proof of the following theorem. Note that henceforth, we use the notation $M = \text{circ}(m_0, m_1, \dots, m_{N-1})$ to denote a circulant matrix with first row $(m_0, m_1, \dots, m_{N-1})$.

Theorem 3.1. *Suppose that a network of N cells has \mathbf{Z}_N symmetry. The only architectures that support two synchronous clusters of adjacent cells of sizes k and $N - k$ are described by coupling matrices of the form*

$$(3.5) \quad A = \text{circ}(\beta_0, \alpha_1, \dots, \alpha_{G-1}, \alpha_0, \alpha_1, \dots, \alpha_{G-1}, \dots, \alpha_0, \alpha_1, \dots, \alpha_{G-1}),$$

where $\beta_0, \alpha_0, \dots, \alpha_{G-1} \in \mathbb{N} \cup \{0\}$ and $G = \text{gcd}(k, N)$.

Proof. If Γ is an abelian group and M commutes with Γ , then M can be diagonalized using the irreducible subspaces associated with the action of Γ as a basis. When $\Gamma = \mathbf{Z}_N$, these subspaces can be computed directly and are given in complex coordinates as $V_i = \mathbf{C}(1, \xi^i, \xi^{2i}, \dots, \xi^{(N-1)i})$, where $\xi = \exp(2\pi i/N)$ is the N th root of unity and \mathbf{C} is the field of complex numbers. We can therefore diagonalize M to obtain $\tilde{M} = C^{-1}MC$, where

$$C = \begin{bmatrix} 1 & 1 & 1 & \dots & 1 \\ 1 & \xi & \xi^2 & \dots & \xi^{N-1} \\ 1 & \xi^2 & \xi^4 & \dots & \xi^{2(N-1)} \\ \dots & \dots & \dots & \dots & \dots \\ 1 & \xi^{N-1} & \xi^{2(N-1)} & \dots & \xi^{(N-1)^2} \end{bmatrix}.$$

It is straightforward to compute

$$C^{-1} = \frac{1}{N} \begin{bmatrix} 1 & 1 & 1 & \dots & 1 \\ 1 & \xi^{-1} & \xi^{-2} & \dots & \xi^{-(N-1)} \\ 1 & \xi^{-2} & \xi^{-4} & \dots & \xi^{-2(N-1)} \\ \dots & \dots & \dots & \dots & \dots \\ 1 & \xi^{-(N-1)} & \xi^{-2(N-1)} & \dots & \xi^{-(N-1)^2} \end{bmatrix}.$$

Note that our original problem (3.4) is equivalent to

$$(3.6) \quad [C^{-1}MC]C^{-1}a = \tilde{M}C^{-1}a \in C^{-1}V,$$

where the fact that \tilde{M} is diagonal will simplify subsequent calculations. Direct computation gives

$$C^{-1}MC = \tilde{M} = \text{diag} \left(\sum_{i=0}^{N-1} m_i, \sum_{i=0}^{N-1} m_i \xi^i, \sum_{i=0}^{N-1} m_i \xi^{2i}, \dots, \sum_{i=0}^{N-1} m_i \xi^{(N-1)i} \right).$$

In particular, if the circulant matrix in our example has the form $M = \text{circ}(m_0, m_1, \dots, m_{N-1}) = \text{circ}(1, 1, \dots, 1, 0, 0, \dots, 0)$, where the first k entries are 1's, then we have

$$(3.7) \quad \tilde{M} = \text{diag} \left(\sum_{i=0}^{k-1} m_i, \sum_{i=0}^{k-1} m_i \xi^i, \sum_{i=0}^{k-1} m_i \xi^{2i}, \dots, \sum_{i=0}^{k-1} m_i \xi^{(N-1)i} \right)$$

$$(3.8) \quad = \text{diag}(\lambda_0, \lambda_1, \dots, \lambda_{N-1}).$$

The following proposition is easy to check from this form.

Proposition 3.2. *The matrix M has zero eigenvalues only when $G = \gcd(k, N) \neq 1$. If this condition holds, then*

$$\lambda_{\frac{lN}{G}} = \sum_{i=0}^{k-1} \xi^{\frac{lNi}{G}} = 0 \quad \text{for } l = 1, 2, \dots, G-1.$$

Proof. Only when the conditions of the proposition are satisfied are the k complex roots ξ^{mi} equidistributed around the unit circle, so that their center of gravity is 0. ■

It follows from this proposition that the kernel of M has dimension $G-1$. Therefore $M^{-1}V$, where the inverse is meant in a set theoretic sense, has dimension at most $\dim(\ker M) + \dim(V) = G+1$.

Next we compute a . Specifically, we use $\tilde{M}C^{-1}a \in C^{-1}V$, and our goal is to find the vectors of natural numbers a that satisfy this relation. It will be easiest to work in \mathbf{C}^N to obtain the linear space $C\tilde{M}C^{-1}V = M^{-1}V$ and complete the problem by finding the intersection of this space with the lattice of natural numbers.

Since V is a linear subspace, it is sufficient to proceed in two steps. We start by finding the kernel of \tilde{M} and the inverse of R_0w_1 , after which we compute the inverse of S_0w_2 .

Let e_i be the i th unit vector. Since \tilde{M} is diagonal, a direct computation shows that

$$(3.9) \quad \tilde{M}^{-1}C^{-1}(\mathbf{C}w_1) = \mathbf{C}e_0 \oplus \bigoplus_{i=1}^{G-1} \mathbf{C}e_{\frac{iN}{G}}.$$

The right-hand side of (3.9) is written as a sum, since $\mathbf{C}e_0$ is a vector space that is not in the kernel, and gets mapped onto $\mathbf{C}w_1$, while the remainder, $\bigoplus_{i=1}^{G-1} \mathbf{C}e_{\frac{iN}{G}}$, comes from the kernel of \tilde{M} .

We next need to find the image of the subspace in (3.9) under C to determine the space that the coefficients in a can come from. A direct computation gives

$$(3.10) \quad C\tilde{M}^{-1}C^{-1}(\mathbf{C}w_1) = \left\{ \left(\sum_{i=0}^{G-1} c_i \xi^0, \sum_{i=0}^{G-1} c_i \xi^{\frac{iN}{G}}, \sum_{i=0}^{G-1} c_i \xi^{\frac{2iN}{G}}, \dots, \sum_{i=0}^{G-1} c_i \xi^{\frac{miN}{G}}, \dots \right)^T, \right. \\ \left. \text{where } c_0, \dots, c_{G-1} \in \mathbf{C} \right\}.$$

It can be checked directly that in the vector defined on the right-hand side of (3.10), every G th entry is the same. This divides the vector into G equivalence classes. In particular, the following is true.

$$C\tilde{M}^{-1}C^{-1}(\mathbf{C}w_1) \cap (\mathbb{N}^N \cup \{0\}) = \{(\alpha_0, \alpha_1, \dots, \alpha_{G-1}, \alpha_0, \alpha_1, \dots, \alpha_{G-1}, \alpha_0, \dots, \alpha_1, \dots, \alpha_{G-1})^T, \\ \text{where } \alpha_0, \dots, \alpha_{G-1} \in (\mathbb{N} \cup \{0\})\}.$$

For the second step, a similar argument can be used to obtain $C\tilde{M}^{-1}C^{-1}(\mathbf{C}w_2)$, but it is sufficient to notice that $M(\mathbf{C}e_0) = \mathbf{C}w_2$, so that the space that we are missing is just $\mathbf{C}e_0$, where $e_0 = (1, 0, 0, \dots, 0)^T$.

This completes the computation and shows that

$$M^{-1}V \cap (\mathbb{N}^N \cup \{0\}) = \{(\beta_0, \alpha_1, \dots, \alpha_{G-1}, \alpha_0, \alpha_1, \dots, \alpha_{G-1}, \alpha_0, \dots, \alpha_1, \dots, \alpha_{G-1})^T, \\ \text{where } \beta_0, \alpha_0, \dots, \alpha_{G-1} \in (\mathbb{N} \cup \{0\})\}. \quad \blacksquare$$

Since we do not allow architectures in which the only coupling is self-coupling, three simple corollaries follow from this result; the second is a special case of the first.

Corollary 3.3. *If $\gcd(k, N) = 1$, then a balanced coloring requires all-to-all coupling.*

Corollary 3.4. *In a ring of coupled, identical cells, the only way to balance a coloring in which one cell is of one color and all other cells are of a second color is an all-to-all coupling scheme, with possible self-coupling.*

Corollary 3.5. *If the number of connections from any cell to any other cell in a network is constrained to be 0 or 1, then there are at most $4(2^{G-1} - 1)$ architectures and at least $2(2^{G-1} - 1)$ architectures that give a nontrivial balanced coloring.*

Proof. Theorem 3.1 gives 2^{G+1} possible connection architectures. Of these, 4 are trivial (fully uncoupled without self-coupling, fully uncoupled with self-coupling, all-to-all coupled without self-coupling, and all-to-all coupled with self-coupling). Finally, for each of the $4(2^{G-1} - 1)$ that yields disconnected components within the network, there is another architecture in the set for which the network is connected, by Proposition 3.8 below. \blacksquare

Remark 3.1. In the proof of Theorem 3.1, $M^{-1}V$ is computed indirectly by looking at $C\tilde{M}^{-1}C^{-1}V$. As noted in the introduction to this section, and as illustrated in the proof of Theorem 4.1, it is possible to find $M^{-1}V$ directly using the \mathbf{Z}_N structure. In the case of a general abelian group Γ no such tricks are available, and some computation is needed to find the kernel of M . Finding the kernel is much simpler once this matrix is block diagonalized using the irreducible representations of Γ , as was done in the proof of Theorem 3.1.

Remark 3.2. The idea of the proof of Theorem 3.1, leading to the simultaneous solution of a system of linear equations representing relations among numbers of connections, generalizes to polysynchronous solutions incorporating more than two synchronized clusters. To see this, recall that the number m of synchronous clusters is arbitrary in the general notation set up in section 2.2, as can be seen in (2.2) and (2.3). With multiple clusters, multiple connection matrices can be used to ensure that all matrices are circulant; for example, with three clusters, separate matrices can be used to consider inputs from cluster 0 to all other cells, inputs from cluster 1 to all other cells, and inputs from cluster 2 to all other cells, respectively. Thus, the presence of additional clusters adds additional computations.

3.2. An example and remarks on \mathbf{D}_N symmetry. In general, the network architectures we obtain have symmetries that form a subgroup of \mathbf{Z}_N . Rings of cells that are used as models of neuronal networks frequently have reflectional symmetry in addition to \mathbf{Z}_N symmetry. Such networks are \mathbf{D}_N symmetric, and the following is an immediate corollary of the results discussed in the previous section.

Corollary 3.6. *Suppose that a network of N cells has \mathbf{D}_N symmetry. The only architectures that support two synchronous clusters of adjacent cells of sizes k and $N - k$ are described by the coupling matrix*

$$A = \text{circ}(\beta_0, \alpha_1, \dots, \alpha_{G-1}, \alpha_0, \alpha_1, \dots, \alpha_{G-1}, \dots, \alpha_0, \alpha_1, \dots, \alpha_{G-1}),$$

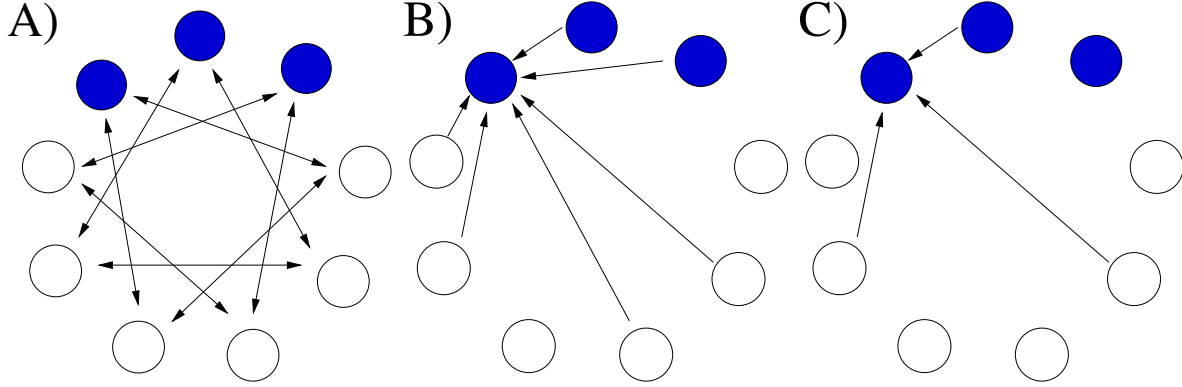


Figure 5. Three balanced colorings of 2 clusters in a network of nine cells. In (a), $a_3 = a_6 = 1$ and $a_i = 0$ for all other i , such that each blue cell receives 2 white inputs and each white cell receives 1 blue input and 1 white input. Interchanging these values (but keeping $a_0 = 0$, corresponding to the absence of self-coupling) yields the architecture in (b), where each cell gets inputs from 4 white cells and 2 blue cells. Both of these have \mathbf{D}_N symmetry (the networks are symmetric under reflection in the line going through one cell and between the two cells on the opposite side of the ring), while the architecture in (c) ($a_1 = a_4 = a_7 = 1$ and $a_i = 0$ for all other i , such that each cell gets inputs from 2 white cells and 1 blue cell) has only \mathbf{Z}_N symmetry. Note that in (b) and (c), connections analogous to those shown are repeated for all cells.

where $\beta_0, \alpha_0, \dots, \alpha_{G-1} \in \mathbb{N} \cup \{0\}$, $G = \gcd(k, N)$, and

$$\alpha_{G-j} = \alpha_j, \quad j = 1, \dots, G-1.$$

Proof. If A commutes with the elements of \mathbf{D}_N , then it is circulant and satisfies $A^T = A$. The result follows immediately. ■

Example. Consider the case $N = 9$, $k = 3$, so that $G = 3$. If we first assume that the network has only \mathbf{Z}_9 symmetry, then Theorem 3.1 implies that

$$(3.11) \quad M^{-1}V \cap (\mathbb{N}^9 \cup \{0\}) = \{(\beta_0, \alpha_1, \alpha_2, \alpha_0, \alpha_1, \alpha_2, \alpha_0, \alpha_1, \alpha_2)^T, \text{ where } \beta_0, \alpha_0, \alpha_1, \alpha_2 \in (\mathbb{N} \cup \{0\})\}.$$

Therefore, $a_0 = \beta_0$, $a_1 = a_4 = a_7 = \alpha_1$, $a_2 = a_5 = a_8 = \alpha_2$, and $a_3, a_6 = \alpha_0$. If we also impose \mathbf{D}_9 symmetry, then

$$(3.12) \quad M^{-1}V \cap (\mathbb{N}^9 \cup \{0\}) = \{(\beta_0, \alpha_1, \alpha_1, \alpha_0, \alpha_1, \alpha_1, \alpha_0, \alpha_1, \alpha_1)^T, \text{ where } \beta_0, \alpha_0, \alpha_1 \in (\mathbb{N} \cup \{0\})\}.$$

To satisfy (3.12) nontrivially, we can let $a_3 = a_6 = 1$ and set the rest of the coefficients in A to 0. This will lead to the coloring shown in Figure 5A. A closer inspection of this solution shows that this network is not connected and consists of three smaller subnetworks of three cells, as shown in Figure 4. The other nontrivial balanced coloring that satisfies (3.12) comes from the complementary network $a_1 = a_4 = a_7 = 1$ and $a_2 = a_5 = a_8 = 1$, with $a_0 = a_3 = a_6 = 0$; see Figure 5B. The only other option that satisfies (3.12) is an all-to-all coupled network. There are several options that satisfy (3.11) but not (3.12), corresponding to \mathbf{Z}_N but not \mathbf{D}_N symmetry. An example appears in Figure 5C.

3.3. Connected networks. As shown in both preceding examples, certain solutions to the given problem are trivial, since they result in networks that contain disconnected components. A network will be connected if and only if its connectivity matrix A is irreducible. Since $A \geq 0$ (that is, all of its elements are nonnegative), the irreducibility of A is equivalent to the positivity of $(I + A)^{N-1}$, where I is the N by N identity matrix [19], a condition which can be checked directly.

It is also useful to think of the directed graph (*digraph*) associated with the network, formed by taking each cell as a node and each connection as an edge. Because we consider coupling architectures with \mathbf{Z}_N symmetry, the digraph obtained this way is *regular*, meaning that each node has the same number of incoming edges as all other nodes; indeed, this follows from the fact that the connection matrix A is circulant. Since A is circulant, one of its eigenvalues is given by $\lambda^* = \sum_{j=0}^{N-1} a_{ij} = \beta_0 + (N/G - 1)\alpha_0 + (N/G)(\alpha_1 + \dots + \alpha_{G-1})$ [6]. A well-known result from graph theory states that the number of connected components in the digraph associated with A is exactly the algebraic multiplicity $am(\lambda^*)$ of the eigenvalue λ^* [5]. Thus, our network is connected if and only if $am(\lambda^*) = 1$.

An alternative derivation of a necessary and sufficient criterion for connectedness comes from a direct consideration of the network. Recall that in the labeling system we have used, within connectivity matrix A , the element $a_{0,j}$, $j = 0, \dots, N-1$, denotes the number of connections to cell 0 from the cell located j places away from it in the ring in an arbitrarily selected but fixed direction. Similar interpretations hold for $a_{i,j}$, $i \neq 0$, but we focus on $i = 0$ since we have assumed \mathbf{Z}_N symmetry and A is thus circulant. By this \mathbf{Z}_N symmetry, the network is connected if there exists $j \in \{0, \dots, N-1\}$ such that j is relatively prime to N and $a_{0,j} \neq 0$. This follows immediately from the fact that if j, N are relatively prime, then the least common multiple of j and N is jN . In terms of the graph of the network, when such j exists, if we start at cell 0 and follow connections of length j in the specified direction, we will reach every other cell in the network before returning to cell 0. One special case is $\alpha_1 \neq 0$, corresponding to nearest neighbor coupling, which always fully connects the network, since $j = 1$ is relatively prime to every N .

The above criterion is not necessary; for example, in a network of $N = 12$ cells, full connectivity is achieved if $\alpha_0 = 0 = \alpha_1$ and $\alpha_2 \neq 0 \neq \alpha_3$, although neither 2 nor 3 is relatively prime to 12. However, this criterion generalizes to the following necessary and sufficient condition for connectedness.

Proposition 3.7. *Assume that a network of N cells has coupling matrix given by $A = \text{circ}(a_0, a_1, \dots, a_{N-1})$ and consider a polysynchronous state with clusters of sizes $k, N-k$, such that $G = \text{gcd}(k, N) \neq 1$. For $j = 1, \dots, N-1$, let $\gamma_j = j$ if $a_j \neq 0$, and let $\gamma_j = 0$ if $a_j = 0$. The network is connected if and only if there exist nonnegative integer coefficients n_1, \dots, n_{N-1} such that*

$$(3.13) \quad \sum_{i=1}^{N-1} n_i \gamma_i \equiv 1 \pmod{N}.$$

Proof. First, consider whether there exists a path in the network from cell 1 to cell 0. Let $J = \{j \in 1, \dots, N-1 : a_j \neq 0\}$. Note that if a path from cell 1 to cell 0 exists, then it consists of a sequence of connections of lengths that appear in J . If we choose n_j as the number of

times that a connection of length j appears in this path, for each $j \in J$, then this choice yields a solution of (3.13), with n_j chosen arbitrarily for those j not in J .

Similarly, suppose that (3.13) has a solution (n_1, \dots, n_{N-1}) . In this case, starting from cell 1 and following n_j paths of length j , for each $j \in J$, yields a path from cell 1 to cell 0 composed of connections that do appear in the network architecture.

In summary, (3.13) has a solution (n_1, \dots, n_{N-1}) if and only if there exists a path in the network from cell 1 to cell 0. Thus, when the network is connected, (3.13) has a solution, and when (3.13) has a solution, applying the network's \mathbf{Z}_N symmetry yields a path from every other cell in the network to cell 0, such that the network is connected. ■

Remark 3.3. Note that with \mathbf{Z}_N symmetry, such that A is given by (3.5), the γ_j above are interrelated. In such a case, Proposition 3.7 can of course be rewritten using the elements α_j to define the terms γ_j . It does not, however, suffice to consider only $\gamma_1, \dots, \gamma_{G-1}$. For example, if $N = 12$ and $G = 3$, then 2 divides N , but $a_{0,5} = a_{0,2} = \alpha_2$, so the condition $\alpha_2 \neq 0$ is enough to ensure that (3.13) can be satisfied. That is, even though $2n \not\equiv 1 \pmod{12}$ for each nonnegative integer n , we have $5n \equiv 1 \pmod{12}$ for an appropriate choice of n , such as $n = 5$.

Finally, we note that while we consider disconnected architectures to be trivial, finding one is still useful, as the following proposition specifies.

Proposition 3.8. *If a pattern of synchrony is supported by a disconnected, but not completely uncoupled, architecture, then there exists a nontrivial connected architecture that supports it as well.*

Proof. For any choice of $\{\beta_0, \alpha_0, \alpha_1, \dots, \alpha_{G-1}\}$ that satisfies (3.5), all complementary architectures, attained by making all nonzero elements zero and vice versa, also satisfy (3.5). Since the network has \mathbf{Z}_N symmetry, it is easy to see that the complement of a disconnected network is connected. In particular, if a network is disconnected, then $a_{0,N-1} = 0 = a_{i,i+1}$ for $i = 0, \dots, N-2$. It follows that in the complementary network, $a_{0,N-1} = a_{i,i+1} = 1$, and since nearest neighbors are coupled, the network must be connected. Similarly, choosing any nonzero values for $a_{0,N-1}$ and $a_{i,i+1}$ yields a connected network. These connected networks will be nontrivial (i.e., not coupled all-to-all) as long as the original network is not fully uncoupled. ■

Remark 3.4. In fact, the complement of a disconnected network is connected in arbitrary networks, without the assumption of \mathbf{Z}_N symmetry, by an analogous argument.

4. Rings of cells of two types. We next develop a general theory for synchrony in rings of cells of two types. As an example, consider the network in Figure 6. There are two alternating types of cells in this ring; we can think of the round cells as E cells and the rectangular cells as I cells. The cells are further subdivided into four synchronous groups. We will refer to this architecture as a *double ring*. Note that although the cells of different types are shown as being interleaved in Figure 6, and this arrangement is assumed in our presentation, the results we obtain below (see Theorem 4.1) apply for any pair of interacting cell groups such that each set of connections (whether between groups or within a group) features \mathbf{Z}_N symmetry, regardless of their actual spatial arrangement.

As discussed previously, all cells in a synchronous group will be referred to as having the same color. Our goal is to describe the architectures that will support an activity pattern in which groups of k and $N - k$ adjacent E cells and l and $N - l$ adjacent I cells evolve

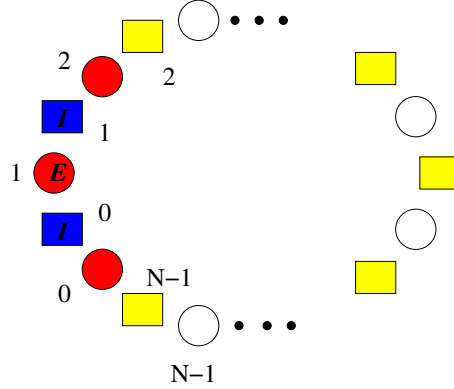


Figure 6. A ring network with two cell types, E and I . Cells of each type are numbered from 0 up to $N-1$, increasing in the clockwise direction, and each cell population is subdivided into two clusters, as shown.

synchronously, with adjacency defined relative only to cells of the same type (see Figure 6). Note that the four clusters of adjacent cells can be located anywhere around the ring; Figure 6 shows one possible cell arrangement with $k = 3$ and $l = 2$.

In general, we cannot expect cells to be exactly synchronous unless they are of the same type. Two E or I cells can be expected to be synchronous only if their input sets are identical [24, 13]. This situation is a direct generalization of the one described in section 2.2, with the exception that there are two input sets \mathcal{C}_i^E and \mathcal{C}_i^I into each cell, corresponding to the two types of cells in the networks. Two cells of the same type can exhibit robust synchrony only when there are bijections $\phi^E : \mathcal{C}_i^E \rightarrow \mathcal{C}_j^E$ and $\phi^I : \mathcal{C}_i^I \rightarrow \mathcal{C}_j^I$ that carry the inputs to cell i from each synchronous group to inputs to cell j from the same group.

Denote the connectivity matrices between the E cells and the I cells by A^{EE} and A^{II} , respectively (these matrices connect cells of equal type). In addition, the matrices A^{EI} and A^{IE} will represent connections from I to E cells and from E to I cells, respectively. As in the previous section, if we assume that the network has \mathbf{Z}_N symmetry, then all of these matrices are circulant. For example, $A^{EE} = \text{circ}(a_0^{EE}, a_1^{EE}, \dots, a_{N-1}^{EE})$, since there are N E cells. The cells in the network are numbered by assigning the first cell in the group of k synchronous E cells the number 0, and proceeding clockwise. The I cells are numbered similarly (see Figure 6).

Let R^0, R^1, R^2 , and R^3 be 4-vectors that denote the total number of inputs to each of the different cell types, where the labels 0, 1, 2, and 3 denote red and white E cells and blue and yellow I cells respectively. For instance, R_1^0 is the total number of inputs to the red E cells from the white E cells. Similarly, let $e_0 = \dots = e_{k-1} = (1, 0, 0, 0)^T$, $e_k = \dots = e_{N-1} = (0, 1, 0, 0)^T$ and $d_0 = \dots = d_{l-1} = (0, 0, 1, 0)^T$, $d_l = \dots = d_{N-1} = (0, 0, 0, 1)^T$ denote the cells in the two different groups, as in the previous section.

The condition that the input sets of two E cells sharing the same color are equivalent leads to the set of equations

$$(4.1) \quad \begin{aligned} a_0^{EE} e_0 + \dots + a_{N-1}^{EE} e_{N-1} + a_0^{EI} i_0 + \dots + a_{N-1}^{EI} i_{N-1} &= R^0 \\ a_{N-1}^{EE} e_0 + \dots + a_{N-2}^{EE} e_{N-1} + a_{N-1}^{EI} i_0 + \dots + a_{N-2}^{EI} i_{N-1} &= R^0 \end{aligned}$$

$$\dots$$

$$a_1^{EE}e_0 + \dots + a_0^{EE}e_{N-1} + a_1^{EI}i_0 + \dots + a_0^{EI}i_{N-1} = R^1,$$

where R^0 appears on the right-hand side in the first k equations and R^1 appears on the right-hand side in the next $N - k$ equations. A similar set of equations, involving the matrices A^{IE} and A^{II} , holds for the I cells.

This set of equations (4.1) splits into two independent groups. Note that for the matrices A^{EE} and A^{II} we obtain equations that are equivalent to (3.1). This observation follows directly from the way the problem is set up: the E to E and I to I connections that support a given pattern of synchrony are determined independently of the other connections in the network. Therefore Theorem 3.1 can be used directly to determine the structure of these matrices.

For the connections from the I to the E cells, we obtain from (4.1) the equations

$$(4.2) \quad \begin{array}{ll} a_0^{EI} + a_1^{EI} + \dots + a_{l-1}^{EI} = R_2^0 & a_l^{EI} + \dots + a_{N-1}^{EI} = R_3^0 \\ \dots & \dots \\ a_{N-k+1}^{EI} + a_{N-k+2}^{EI} + \dots + a_{N-k+l}^{EI} = R_2^0 & a_{N-k+l+1}^{EI} + \dots + a_{N-k}^{EI} = R_3^0 \\ a_{N-k}^{EI} + a_{N-k+1}^{EI} + \dots + a_{N-k+l-1}^{EI} = R_2^1 & a_{N-k+l}^{EI} + \dots + a_{N-k-1}^{EI} = R_3^1 \\ \dots & \dots \\ a_1^{EI} + a_2^{EI} + \dots + a_l^{EI} = R_2^1 & a_{l+1}^{EI} + \dots + a_0^{EI} = R_3^1. \end{array}$$

As in the case of (3.1), the left and right columns are equivalent. As in section 3.1, we reorder the equations from the left column and put the first equation first, and then follow with the last equation up to the second equation. Once reordered, we have

$$(4.3) \quad Ma^{EI} = R,$$

where

$$(4.4) \quad a^{EI} = (a_0^{EI}, a_1^{EI}, \dots, a_{N-1}^{EI})^T,$$

$$(4.5) \quad R = (R_2^0, \underbrace{R_2^1, \dots, R_2^1}_{N-k \text{ times}}, R_2^0, \dots, R_2^0)^T,$$

and

$$(4.6) \quad M = \begin{bmatrix} 1 & 1 & 1 & \dots & 1 & 0 & 0 & \dots & 0 & 0 \\ 0 & 1 & 1 & \dots & 1 & 1 & 0 & \dots & 0 & 0 \\ 0 & 0 & 1 & \dots & 1 & 1 & 1 & \dots & 0 & 0 \\ & & & \dots & & & & \dots & & \\ 1 & 1 & 1 & \dots & 0 & 0 & 0 & \dots & 0 & 1 \end{bmatrix},$$

where each row contains $N - l$ zero entries. We obtain the same equation for the matrix A^{IE} , with the roles of k and l reversed.

The problem of solving (4.3) is virtually identical to that of solving (3.2) with (3.3). The difference, which somewhat complicates the calculations, is that in the present case k does not necessarily equal l .

Theorem 4.1. *Suppose that a network composed of N E cells and N I cells forms a double ring and that groups of k and $N - k$ adjacent E cells and l and $N - l$ adjacent I cells form synchronous clusters. Let $G_k = \gcd(k, N)$ and $G_l = \gcd(l, N)$. The connectivity matrices that can support this form of synchrony between identical cells are given by*

$$A^{EE} = \text{circ}(\beta_0^{EE}, \alpha_1^{EE}, \dots, \alpha_{G_k-1}^{EE}, \alpha_0^{EE}, \alpha_1^{EE}, \dots, \alpha_{G_k-1}^{EE}, \dots, \alpha_0^{EE}, \alpha_1^{EE}, \dots, \alpha_{G_k-1}^{EE}),$$

$$A^{II} = \text{circ}(\beta_0^{II}, \alpha_1^{II}, \dots, \alpha_{G_l-1}^{II}, \alpha_0^{II}, \alpha_1^{II}, \dots, \alpha_{G_l-1}^{II}, \dots, \alpha_0^{II}, \alpha_1^{II}, \dots, \alpha_{G_l-1}^{II}),$$

where all entries are in $\mathbb{N} \cup \{0\}$.

The connectivity matrix A^{EI} has the form

$$A^{EI} = \text{circ}(\beta_0^{EI}, \alpha_1^{EI}, \dots, \alpha_{G_l-1}^{EI}, \beta_{G_l}^{EI}, \alpha_1^{EI}, \dots, \alpha_{G_l-1}^{EI}, \beta_{2G_l}^{EI}, \dots, \beta_{N-G_l}^{EI}, \alpha_1^{EI}, \dots, \alpha_{G_l-1}^{EI}).$$

If $k \equiv 0 \pmod{G_l}$, then the coefficients $\beta_0, \beta_l, \beta_{2l}, \dots$ split into two equivalence classes

$$(4.7) \quad \begin{aligned} \beta_l &= \beta_{2l} = \dots = \beta_{N-k}, \\ \beta_{N-k+l} &= \beta_{N-k+2l} = \dots = \beta_0, \end{aligned}$$

where all subscripts are taken modulo N . If $k \not\equiv 0 \pmod{G_l}$, then there is only one equivalence class

$$\beta_l = \beta_{2l} = \dots = \beta_0.$$

The same holds for A^{IE} with the roles of k and l reversed.

Remark 4.1. If $k = l$, so that the two clusters contain the same number of cells, then, since $N - k + l = N$, the sets of matrix entries in (4.7) are composed of β_0 in one class and the remaining entries in the second. The matrix A^{EI} has, therefore, the same form as A^{EE} and A^{II} in this case. However, note that the coefficient $a_0^{EI} = \beta_0^{EI}$ gives the number of connections from the j th I cell to the j th E cell, while a_0^{EE} and a_0^{II} give the number of self-couplings of each E and I cell, respectively.

Proof. We need to find solutions to four problems of the form

$$(4.8) \quad Ma \in V,$$

where

$$V = R w_1 \oplus S w_2 \stackrel{\text{def}}{=} R(1, 1, 1, \dots, 1)^T \oplus S(1, 0, 0, \dots, 0, 1, 1, \dots, 1)^T.$$

The number of zeros in a row of M and in w_2 both equal $N - k$ and $N - l$ in the cases of A^{EE} and A^{II} , respectively, and therefore Theorem 3.1 can be applied directly.

In the case of A^{EI} , the matrix M has $N - l$ zero entries, while w_2 has $N - k$ zero entries. Since w_1 and M have the same form as in section 3.1, we can proceed as in the proof of Theorem 3.1 to find $C\tilde{M}^{-1}C^{-1}(Cw_1)$ and obtain the same result as in (3.10).

A similar argument can be used to obtain $C\tilde{M}^{-1}C^{-1}(\mathbf{C}w_2)$, although the calculations are lengthy. Rather than providing these calculations, we provide a short proof, which uses the \mathbf{Z}_N symmetry of the system directly.

We will use the structure of the left column in (4.2), which determines all possible values for a^{EI} . Suppose that the right-hand sides of two adjacent equations are equal. Then subtracting the two equations leads to $a_j^{EI} = a_{j-l}^{EI}$ for some j , where the indices are taken modulo N . We therefore obtain all equations of the form $a_j^{EI} = a_{j-l}^{EI}$, except for two. The two missing equations are

$$(4.9) \quad a_0^{EI} = a_l^{EI} \quad \text{and} \quad a_{N-k}^{EI} = a_{N-k+l}^{EI}.$$

If these equalities were included with the remaining $N - 2$ equalities, the coefficients a_j^{EI} would form $G_l = \gcd(l, N)$ equivalence classes. Each set of equalities defining an equivalence class would form a “ring,” in the sense that

$$(4.10) \quad a_j^{EI} = a_{j+l}^{EI} = \dots = a_{j+\frac{lN}{G_l}}^{EI} = a_j^{EI}.$$

Therefore, it is necessary to remove more than one equality defining this equivalence class to split it into two classes. That is, the coefficients $\beta_0, \beta_l, \beta_{2l}, \dots$ split into two classes, as described in (4.7), if and only if the equalities in (4.9) both come from the same “ring” of equations defined by (4.10).

Since N and l are both multiples of G_l , it can now be easily checked that if $k \not\equiv 0 \pmod{G_l}$, then the equality $a_{N-k}^{EI} = a_{N-k+l}^{EI}$ is not in the set of equalities defining the equivalence class of a_0^{EI} , and there are G_l equivalence classes for the coefficients. On the other hand, if $k \equiv 0 \pmod{G_l}$, then removing the two equalities (4.9) breaks the equivalence class of a_0^{EI} into two in the way described in (4.7). ■

From the proof of Theorem 4.1, it is clear that Theorem 4.1 holds regardless of where the l I cells are positioned relative to the k E cells; adjacency of the clusters is not needed. The lengths of the connections corresponding to the elements of the connection matrix depend on these positions, however, so application of the theorem implies that different relative cluster positions will be supported by different coupling architectures.

Example. Consider again the example of $N = 7$ discussed in section 2.3. In the case of a double ring of 7 E cells and 7 I cells, $G_k = G_l = 1$ for any choice of k, l . Thus, A^{EI} is a 7 by 7 matrix of the form $A^{EI} = \text{circ}(\beta_0^{EI}, \beta_1^{EI}, \dots, \beta_6^{EI})$. Suppose, for example, that $k = 3$, as in Figure 1, such that $k \equiv 0 \pmod{G_l}$ and (4.7) applies. If $l = 2$, then (4.7) yields

$$(4.11) \quad \beta_2 = \beta_4, \quad \beta_6 = \beta_1 = \beta_3 = \beta_5 = \beta_0.$$

Equation (4.11) gives rise to two nontrivial (and complementary) architectures of I to E connections, each corresponding to setting the elements of one of the equivalence classes of connections equal to 1 and setting the other class equal to 0. These are displayed in Figure 7A, B; the second of these also appears in Figure 1. Interestingly, if $l = N - 2 = 5$, then we get different equivalence classes, namely,

$$(4.12) \quad \beta_5 = \beta_3 = \beta_1 = \beta_6 = \beta_4, \quad \beta_2 = \beta_0.$$

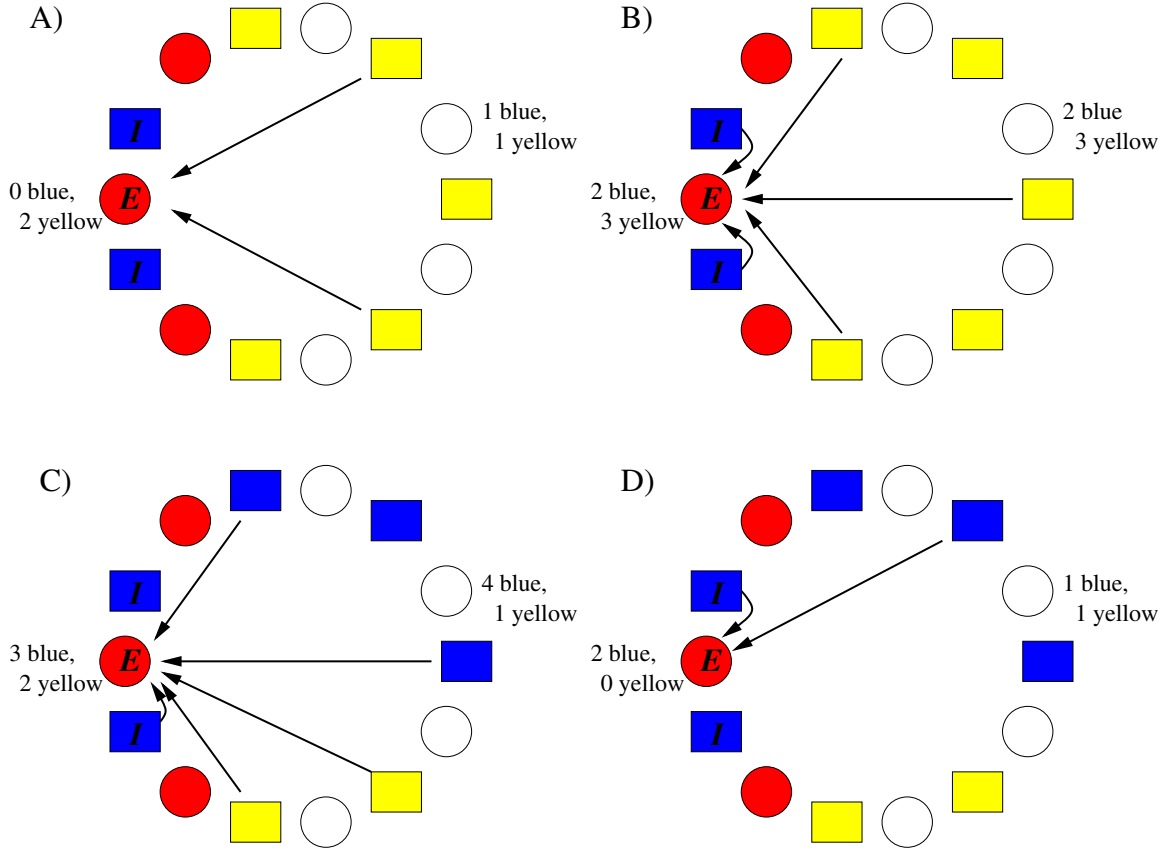


Figure 7. Architectures of I to E connections yielding balanced colorings in a ring of 7 E cells and 7 I cells, grouped in 4 clusters. In each figure, we show only the connections to a particular E cell, but each E cell receives an analogous pattern of inputs as dictated by \mathbf{Z}_N symmetry. The text indicates the number of each connection type received by each E cell in each cluster (all E cells of the same color receive the same number of each connection type since these are balanced colorings). The top figures correspond to the equivalence classes for $l = 2$, given in (4.11), with $\beta_2 = \beta_4 = 1$, $\beta_6 = \beta_1 = \beta_3 = \beta_5 = \beta_0 = 0$ in (a) and $\beta_2 = \beta_4 = 0$, $\beta_6 = \beta_1 = \beta_3 = \beta_5 = \beta_0 = 1$ in (b). The bottom figures correspond to the equivalence classes for $l = 5$, given in (4.12), with $\beta_5 = \beta_3 = \beta_1 = \beta_6 = \beta_4 = 1$, $\beta_2 = \beta_0 = 0$ in (c) and $\beta_5 = \beta_3 = \beta_1 = \beta_6 = \beta_4 = 0$, $\beta_2 = \beta_0 = 1$ in (d).

The two corresponding nontrivial architectures of I to E connections derived from (4.12) are shown in Figure 7C, D.

The case of $l = 5$ leads to different architectures from those arising in the case of $l = 2$, even though $5 = 7 - 2$, because the results of Theorem 4.1 are derived by assuming that the clusters of k E cells and l I cells are aligned as shown in Figure 6. As noted earlier, analogous results to Theorem 4.1 can be derived for other relative positions of these clusters, using the same methods. As one of the clusters is moved around the ring, the numbering changes, and, although one obtains the same solution in terms of coupling matrix coefficients, the architectures will look different.

Of course, by switching the labels on the cells in this example, we can attain a balanced coloring with a nontrivial coupling architecture for polysynchronous states with E cell clusters

of sizes 2 and 5 and I cell clusters of sizes 3 and 4. As noted earlier, E cell clusters of sizes 3 and 4, or of sizes 2 and 5, would only be possible with trivial coupling architectures in a single ring of 7 E cells, by Corollary 3.3.

5. Discussion. Coupling architecture is frequently crucial in determining the dynamical behavior of a coupled network. To model a collection of interacting cells, it is therefore necessary to have accurate information about the ways in which the cells interact. Unfortunately, in areas such as experimental neuroscience, such information may be very difficult to obtain directly.

The method we presented provides a means of determining possible network architectures based on observed activity patterns. The architectures obtained using this analysis are the only ones within their class that can support the given activity patterns robustly, without the presence of specialized features in the intrinsic dynamics of the cells in the network. Clearly, this inverse approach is meant to complement, not replace, consideration of details of cellular and coupling dynamics, which are known to play a very important role in determining the activity patterns manifested in networks.

In particular, the information we derive could be useful in selecting coupling architectures to use in models of networks known to produce certain activity patterns, in designing novel networks to produce particular activity patterns, or in deducing the actual architectural properties of physical networks. Note that in the former two applications, the network size N would be known or selectable, while in the latter case, knowledge about N would depend on the particular physical network under consideration.

Without imposing certain assumptions, the architectural constraint problem becomes too general. It is important to restrict to a general class of architectures to start the process, in order to narrow the number of possibilities and eliminate trivialities. In the examples considered, although the network size N could be arbitrary, this restriction was given by the requirement that the network have \mathbf{Z}_N or \mathbf{D}_N symmetry.

Networks of interacting cells with \mathbf{Z}_N symmetry in the coupling architecture are frequently used as models of neuronal systems; however, the method we present can be generalized in many ways. The description of polysynchronous states, given in section 2.2, is valid even in nonsymmetric networks. The approach given in the proof of Theorem 3.1 can be generalized to any network whose symmetries are given by an abelian group. We believe that a similar approach is valid more generally, although current representation theory would have to be extended to deal with such cases.

It was shown in section 4 that the method can be extended to networks with multiple types of cells. One result of this extension is that, given a particular network of cells, coupling a second group of cells to the first can greatly expand the range of architectures that can balance a particular coloring of the original cells. If a network of one cell type has N cells with $\gcd(k, N) = 1$, then a 2-cluster state with clusters of sizes k and $N - k$ will be balanced if and only if the network is uncoupled or all-to-all coupled; however, synchrony is never stable in uncoupled systems. Our results show that under fairly general conditions (see Theorem 4.1), if N cells of a second type are coupled to the original cells, then a balanced coloring featuring the same two clusters in the original cells can be achieved by leaving the original cells uncoupled but coupling the cell types together in a nontrivial way. Such coupling across types can

infer stability on synchronized states (e.g., [27, 23, 22, 18]). More generally, the possibility of connections between two cell types tends to allow for a greater variety of architectures that support particular polysynchronous states. In addition to multiple cell types, similar ideas to those presented here can be used to treat networks with multiple arrow types (in which identical cells may not interact in identical ways) and multiple connections between cells.

In all of the solutions considered, cells in the same cluster are assumed to be adjacent to each other (relative to other cells of the same type) in the ring. In a particular system, this adjacency need not correspond to actual physical proximity. In the mammalian visual cortex, for example, a natural ring structure can be defined in terms of cells' orientation preferences, rather than their spatial positions. Our results apply as long as, once the cells are ordered according to some criterion, the coupling architecture features \mathbf{Z}_N symmetry. Nonetheless, it would be of interest to extend our results to clustered solutions with nonadjacent elements, such as traveling waves on a ring, in which cells a certain wavelength apart in the ring activate together, followed by their neighbors to one side, and so on, until the pattern repeats.

Finally, although we did not discuss the stability of the invariant subspaces corresponding to the polysynchronous states that we study, in certain examples the techniques developed in [1, 2] will be applicable. The invariant subspaces corresponding to different polysynchronous patterns can be nested, exactly as in the case in which the polysynchronous states in a network are determined by symmetry [4, 1, 2]. The network architecture determines the invariant subspaces and how they are nested. In this situation, synchrony breaking bifurcations can occur as a polysynchronous solution bifurcates to another contained in an invariant subspace of higher dimension (a simple example is the transition from a fully synchronous, i.e., a one color solution, to a two color solution). Such transitions correspond to symmetry breaking bifurcations in equivariant bifurcation theory, although in the present case neither the bifurcating nor the resulting solutions need to be symmetric. Stability of polysynchronous states derived from symmetry considerations is also considered in [21], where the specific assumption of diffusive coupling allows for the use of a control theoretic framework in the derivation of stability conditions.

Acknowledgments. We thank Martin Golubitsky for helping to get this work started and for many helpful discussions and comments. Jonathan Rubin also thanks E. Glen Whitehead for suggestions on some useful references in algebraic graph theory.

REFERENCES

- [1] V. BELYKH, I. BELYKH, AND M. HASLER, *Hierarchy and stability of partially synchronous oscillations of diffusively coupled dynamical systems*, Phys. Rev. E (3), 62 (2000), pp. 6332–6345.
- [2] V. N. BELYKH, I. V. BELYKH, AND E. MOSEKILDE, *Cluster synchronization modes in an ensemble of coupled chaotic oscillators*, Phys. Rev. E (3), 63 (2001), 036216.
- [3] H. BERGMAN, A. FEINGOLD, A. NINI, A. RAZ, H. SLOVIN, M. ABELES, AND E. VAADIA, *Physiological aspects of information processing in the basal ganglia of normal and parkinsonian primates*, Trends Neurosci., 21 (1998), pp. 32–38.
- [4] P. C. BRESSLOFF AND S. COOMBES, *Symmetry and phase-locking in a ring of pulse-coupled oscillators with distributed delays*, Phys. D, 126 (1999), pp. 99–122.
- [5] D. CVETKOVIĆ, M. DOOB, AND H. SACHS, *Spectra of Graphs: Theory and Applications*, Academic Press, New York, 1979.

- [6] P. DAVIS, *Circulant Matrices*, John Wiley & Sons, New York, 1979.
- [7] A. DESTEXHE, D. CONTRERAS, AND M. STERIADE, *Mechanisms underlying the synchronizing action of corticothalamic feedback through inhibition of thalamic relay cells*, J. Neurophys., 79 (1988), pp. 999–1016.
- [8] A. DESTEXHE AND T. SEJNOWSKI, *Synchronized oscillations in thalamic networks: Insights from modeling studies*, in *Thalamus*, Volume II, M. Steriade, E. Jones, and D. McCormick, eds., Elsevier, Amsterdam, 1997, pp. 331–372.
- [9] A. ENGEL, P. FRIES, AND W. SINGER, *Dynamic predictions: Oscillations and synchrony in top-down processing*, Nat. Rev. Neurosci., 2 (2001), pp. 704–716.
- [10] M. GOLUBITSKY, M. NICOL, AND I. STEWART, *Some curious phenomena in coupled cell systems*, J. Nonlinear Sci., 14 (2004), pp. 119–136.
- [11] M. GOLUBITSKY, I. STEWART, P. BUONO, AND J. COLLINS, *A modular network for legged locomotion*, Phys. D, 115 (1998), pp. 56–72.
- [12] M. GOLUBITSKY, I. STEWART, P. BUONO, AND J. COLLINS, *Symmetry in locomotor central pattern generators and animal gaits*, Nature, 401 (1999), pp. 693–695.
- [13] M. GOLUBITSKY, I. STEWART, AND A. TÖRÖK, *Patterns of synchrony in coupled cell networks with multiple arrows*, SIAM J. Appl. Dynam. Systems, 4 (2005), pp. 78–100.
- [14] J. HOOVER AND P. STRICK, *The organization of cerebellar and basal ganglia outputs to primary motor cortex as revealed by retrograde transneuronal transport of herpes simplex virus type 1*, J. Neurosci., 19 (1999), pp. 1446–1463.
- [15] J. HOPFIELD AND C. BRODY, *What is a moment? “Cortical” sensory integration over a brief interval*, Proc. Natl. Acad. Sci. USA, 97 (2000), pp. 13919–13924.
- [16] J. HOPFIELD AND C. BRODY, *What is a moment? Transient synchrony as a collective mechanism for spatiotemporal integration*, Proc. Natl. Acad. Sci. USA, 98 (2001), pp. 1282–1287.
- [17] N. KOPELL, G. ERMENTROUT, M. WHITTINGTON, AND R. TRAUB, *Gamma rhythms and beta rhythms have different synchronization properties*, Proc. Natl. Acad. Sci. USA, 97 (2000), pp. 1867–1872.
- [18] S. KUNEC AND A. BOSE, *High-frequency, depressing inhibition facilitates synchronization in globally inhibitory networks*, Network: Comp. Neural Sys., 14 (2003), pp. 647–672.
- [19] H. MINC, *Nonnegative Matrices*, John Wiley & Sons, New York, 1988.
- [20] A. PIKOVSKY, M. ROSENBLUM, AND J. KURTHS, *Synchronization: A Universal Concept in Nonlinear Science*, Cambridge University Press, Cambridge, UK, 2003.
- [21] A. POGROMSKY, G. SANTOBONI, AND H. NIJMEIJER, *Partial synchronization: From symmetry towards stability*, Phys. D, 172 (2002), pp. 65–87.
- [22] J. RUBIN AND D. TERMAN, *Analysis of clustered firing patterns in synaptically coupled networks of oscillators*, J. Math. Biol., 41 (2000), pp. 513–545.
- [23] J. RUBIN AND D. TERMAN, *Geometric analysis of population rhythms in synaptically coupled neuronal networks*, Neural Comput., 12 (2000), pp. 597–645.
- [24] I. STEWART, M. GOLUBITSKY, AND M. PIVATO, *Symmetry groupoids and patterns of synchrony in coupled cell networks*, SIAM J. Appl. Dyn. Syst., 2 (2003), pp. 609–646.
- [25] S. STROGATZ, *Sync: The Emerging Science of Spontaneous Order*, Hyperion, New York, 2003.
- [26] D. TERMAN, J. RUBIN, A. YEW, AND C. WILSON, *Activity patterns in a model for the subthalamopallidal network of the basal ganglia*, J. Neurosci., 22 (2002), pp. 2963–2976.
- [27] D. TERMAN AND D. L. WANG, *Global competition and local cooperation in a network of neural oscillators*, Phys. D, 81 (1995), pp. 148–176.